Published in final edited form as:
Cancer Res. 2008 October 1; 68(19): 7838–7845. doi:10.1158/0008-5472.CAN-08-1899.

Hepatocyte Growth Factor and Sonic Hedgehog Expression in Cerebellar Neural Progenitor Cells Costimulate Medulloblastoma Initiation and Growth

Mandy J. Binning[1,*], **Toba Niazi**[1,*], **Carolyn A. Pedone**[1], **Bachchu Lal**[2,4], **Charles G. Eberhart**[3], **K. Jin Kim**[5], **John Laterra**[2,4], and **Daniel W. Fults**[1]

1*Department of Neurosurgery, University of Utah School of Medicine, Salt Lake City, UT, USA*

2*Department of Neurology, Johns Hopkins School of Medicine, Baltimore, MD, USA*

3*Department of Pathology, Johns Hopkins School of Medicine, Baltimore, MD, USA*

4*Department of Kennedy-Krieger Institute, Johns Hopkins School of Medicine, Baltimore, MD, USA*

5*Galaxy Biotech, LLC; Mountain View, CA, USA*

Abstract

Medulloblastomas are malignant brain tumors that arise by transformation of neural progenitor cells in the cerebellum in children. Treatment-related neurotoxicity has created a critical need to identify signaling molecules that can be targeted therapeutically to maximize tumor growth suppression and minimize collateral neurological injury. In genetically engineered mice, activation of Sonic Hedgehog (Shh) signaling in neural stem cells in the developing cerebellum induces medulloblastomas. Hepatocyte growth factor (HGF) and its cell surface receptor c-Met are highly expressed in human medulloblastomas, and elevated levels of *c-Met* and *HGF* mRNA predict an unfavorable prognosis for patients. HGF is neuroprotective for cerebellar granule cells and promotes growth of human medulloblastoma cells in culture and in murine xenografts. We modeled the ability of HGF to induce medulloblastomas in mice using a version of the RCAS/*tv-a* system that allows gene transfer to cerebellar neural progenitors during their postnatal expansion phase when these cells are highly susceptible to transformation. Here we report a high frequency of medulloblastoma formation in mice after postnatal expression of HGF in cooperation with Shh. Some tumors showed neurocytic differentiation similar to that in human nodular medulloblastomas with activated Shh signaling. Systemic administration of a monoclonal antibody against HGF prolonged survival of mice bearing Shh+HGF—induced medulloblastomas by stimulating apoptosis. These findings indicate a role for HGF in medulloblastoma initiation and growth and demonstrate efficacy of HGF-targeted therapy in a mouse model of endogenously arising tumors.

Keywords

medulloblastoma; hepatocyte growth factor; scatter factor; mouse model; sonic hedgehog

CORRESPONDING AUTHOR: Daniel W. Fults, M.D. Department of Neurosurgery University of Utah School of Medicine 175 North Medical Drive East Salt Lake City, UT 84132, USA. Phone: 801-581-6908 / Fax: 801-581-4385 E-mail: daniel.fults@hsc.utah.edu.
*These authors contributed equally.

Introduction

Medulloblastomas are malignant brain tumors that arise in the cerebellum in children. Aggressive treatment approaches that combine surgery with craniospinal radiation and chemotherapy result in five-year survival rates exceeding 70%, depending on clinical risk factors such as patient age and postsurgical tumor burden (1,2). Despite these encouraging statistics, treatment-related neurotoxicity can cause cognitive impairment, growth retardation, and endocrine dysfunction, as well as psychiatric and behavioral disturbances in long-term survivors. Thus, there is a critical need to enhance treatment specificity by identifying molecular targets that can be exploited to maximize tumor growth suppression and minimize collateral neurological injury.

The use of genetically engineered mice has provided insights into the molecular pathogenesis of medulloblastoma and exposed promising targets for novel therapies. Several different methods of activating the Sonic Hedgehog (Shh) signaling pathway in neural progenitor cells of the developing cerebellum can induce tumors in mice that closely resemble human medulloblastomas. These methods include (a) targeted deletion of the *Patched* gene, which encodes the inhibitory receptor for Shh (3), (b) ectopic expression of Shh by retroviral transfer (4,5), and (c) transgenic overexpression of Smoothened, a positive effector of Shh signaling (6). Moreover, pharmacological inhibition of Shh signaling by an antagonist of Smoothened prolongs survival and promotes regression of medulloblastomas that arise spontaneously in Patched-deficient mice (7).

Although these findings highlight the importance of Shh signaling in the genesis of medulloblastoma, other molecular signals cooperate with Shh to increase tumor penetrance in mice. These include loss of the p53 tumor suppressor (8), stimulation of phosphatidyl inositol 3-kinase (PI3K) signaling by insulin-like growth factor-II (IGF-II) (9), ectopic expression of Myc oncoproteins (5,10), and suppression of apoptosis by Bcl-2 (11).

A large body of experimental evidence from studies of mice and humans indicates that activation of cell signaling by hepatocyte growth factor (HGF), also known as scatter factor, promotes tumor growth. HGF is a multifunctional growth factor that drives cell cycle progression, blocks apoptosis, stimulates cell motility, and promotes angiogenesis (reviewed in (12) and (13)). Overexpression of HGF in transgenic mice via the metallothionein gene promoter, which is constitutively active in many tissues, induces a diverse spectrum of tumor types (14). The physiological effects of HGF are all mediated by its cell surface receptor, the transmembrane tyrosine kinase encoded by the proto-oncogene *c-Met* (15). Transgenic mice in which expression of catalytically activated c-Met receptors is driven by the metallothionein promoter develop mammary carcinomas (16,17). Mice in which expression of wild-type *c-Met* is induced specifically in hepatocytes develop carcinomas of the liver (18). HGF/c-Met signaling is activated in 50% of human solid tumors (www.vai.org/met). HGF and c-Met expression levels correlate with increased malignancy in human gliomas and growth of glioma cell lines can be HGF-dependent (19-21). Nevertheless, it is not known whether aberrant activation of HGF/c-Met signaling in the nervous system can initiate brain tumor formation.

Both *HGF* and *c-Met* are often highly expressed in primary human medulloblastomas, and elevated mRNA levels of these genes predict an unfavorable prognosis for patients (22). HGF is neuroprotective for cerebellar granule cells, which are derived from cells of medulloblastoma origin (23), and HGF stimulates proliferation of granule neuron precursors during normal cerebellar development (24). Furthermore, overexpression of HGF stimulates proliferation of established medulloblastoma cell lines and enhances growth of tumor xenografts in immunodeficient mice (22). These findings suggested to us that HGF might be a potent growth factor for neural progenitor cells *in vivo* and that ectopic expression of HGF in the developing

cerebellum might initiate medulloblastoma formation or cooperate with Shh to promote tumor growth.

To address this question, we used a version of the RCAS/*tv-a* somatic cell gene transfer system that enabled us to express HGF and Shh in nestin-expressing neural progenitors in the cerebellum of postnatal mice. This system uses a replication-competent, avian retroviral vector (RCAS), derived from the avian leukosis virus (ALV subgroup A), and a transgenic mouse line (*Ntv-a*) that produces TV-A (the receptor for ALV-A) under control of the *Nestin* gene promoter (25). Nestin is an intermediate filament protein expressed by neuronal and glial progenitors. When mammalian cells are transduced with RCAS vectors, viral replication does not occur. Instead, the RCAS provirus integrates into the host cell genome, and the transferred gene is expressed as a spliced message under control of the constitutive retroviral promoter, long terminal repeat.

We reported previously that ectopic expression of Shh in this cell population is sufficient to initiate medulloblastoma formation in mice (5). It is likely that the specific cells transformed by Shh hyperstimulation are granule neuron precursors because they comprise the most abundant cell type in the postnatal cerebellum and because they proliferate rapidly in response to physiological levels of Shh (reviewed in (26)). Here we report that ectopic expression of HGF significantly enhances Shh-dependent medulloblastoma formation. Moreover, systemic administration of a neutralizing monoclonal antibody directed against HGF prolonged survival in mice bearing Shh+HGF—induced medulloblastomas. Coupled with the prevalence of HGF/c-Met activation in human tumors, these findings suggest that HGF signaling might be a feasible treatment target in medulloblastoma.

Materials and Methods

Vector construction

The RCAS-HGF vector was constructed by ligating a PCR-generated cDNA corresponding to the complete coding sequence of the human *HGF* gene into the parent retroviral vector RCASBP(A) (27). To detect expression of the retrovirus-transferred protein, we prepared an epitope-tagged version of RCAS-HGF by appending six repeats of the sequence encoding the human c-Myc epitope (EQKLISEEDL), which is recognized by monoclonal antibody 9E10. Construction and characterization of RCAS-Shh, which has six repeats of the influenza virus hemagglutinin (HA) epitope (YPYDVPDYA), has been described previously (5). To produce live virus, we transfected plasmid versions of RCAS vectors into immortalized chicken fibroblasts (DF-1 cells) and allowed them to replicate in culture.

In vivo somatic cell transfer in transgenic mice

Production of the *Ntv-a* transgenic mouse line has been described previously (25). The mice used in these experiments were mixtures of the following strains: C57BL/6, BALB/C, FVB/N, and CD1. To transfer genes via RCAS vectors, we injected retrovirus packaging cells (DF-1 cells transfected with and producing recombinant RCAS retrovirus) into the lateral cerebellum from an entry point just posterior to the lambdoid suture of the skull (10^5 cells in 1–2 μl of PBS). For experiments in which somatic cell transfer of both HGF and Shh was the goal, the cell pellet was prepared by mixing equal numbers of both retrovirus-producing cells. We injected mice within 72 hours after birth because the pool of nestin-positive cells producing ALV-A receptors diminishes progressively afterward. The mice were sacrificed as soon as they showed signs of increased intracranial pressure (indicated by increased head circumference) or debilitation. Asymptomatic mice were sacrificed at the chosen experimental endpoints. The brains were fixed in formalin, divided into quarters by parallel incisions in the coronal plane, embedded in paraffin, and sectioned for immunohistochemical analysis. We estimated tumor

size by tracing tumor circumference from digitized photomicrographs of hematoxylin and eosin (H&E)—stained brain sections and calculated cross-sectional area using Zeiss Axiovision image analysis software.

Immunocytochemistry

To analyze protein expression in tissue sections, we used an immunoperoxidase staining method described previously (5). Briefly, tissue sections (4 μm) were deparaffinized, rehydrated, and then autoclaved in a citrate-based antigen retrieval solution (Vector Laboratories, Burlingame, CA) for 30 min before application of primary antibody. Immunoreactive staining was visualized using an avidin-biotin complex technique with diaminobenzidine as the chromogenic substrate (reddish brown color) and toluidine blue as a nuclear counterstain. We used the following monoclonal antibodies (and dilutions) from the indicated commercial sources: 9E10 (1:50) — human c-Myc (Santa Cruz Biotechnology, Santa Cruz, CA); F7 (1:50) — HA (Santa Cruz); 2F11 (1:100) — 70-kDa neurofilament protein (Dako, Carpinteria, CA); TuJ1 (1:400) — βIII tubulin (Research Diagnostics, Flanders, NJ); Mab377 (1:100) — NeuN (Chemicon, Temecula, CA). We used polyclonal antibodies to detect expression of glial fibrillary acidic protein (GFAP) (1:1000) (Dako).

Assays for proliferation, apoptosis, and microvascular density

Apoptosis was quantified by immunostaining formalin-fixed, paraffin-embedded tissue sections with an antibody against cleaved caspase-3 (Asp175) according to the manufacturer's protocol (Cell Signaling Technology, Danvers, MA). To calculate the apoptotic index, we counted caspase-3—positive cells in 10 contiguous 40x microscope fields (>2×10^3 cells counted) and averaged the percentage of positive cells from 10 different tumors. Proliferation index was determined by the same method using a polyclonal antibody (1:1000) against cell cycle protein Ki67 (Vector Laboratories). To measure microvascular density, we visualized blood vessel walls by immunostaining with a polyclonal antibody (1:50) against laminin (Sigma-Aldrich, St. Louis, MO) and then calculated total vessel area as a percentage of tumor cross-sectional area from digitized photomicrographs.

Reverse transcriptase-polymerase chain reaction (RT-PCR)

Cerebella were removed from euthanized mice and frozen immediately in liquid nitrogen. Tissue specimens were homogenized in Trizol, and total RNA was extracted using RNeasy Mini Kit (Qiagen, Valencia, CA) according to the manufacturer's instructions. RT-PCR was carried out using the SuperScript III One-Step RT-PCR kit (Invitrogen, Carlsbad, CA). In brief, cDNA was synthesized from total RNA by reverse transcription and PCR in the presence of oligonucleotide primers specific for human *HGF*. RT-PCR products corresponding to the constitutively expressed, glycolytic enzyme glyceraldehyde-3-phosphate dehydrogenase (GAPDH) served as internal controls for sample variation in mRNA degradation and gel loading. PCR products were separated by electrophoresis through agarose gels and visualized by ultraviolet illumination after immersion in ethidium bromide solution. Primer sequences were 5′-GTTCCATGATACCACACG-3′ and 5′-GATAACTCTCCCCATTGC-3′ for *HGF* and 5′-GGTGAAGGTCGGAGTCAACG-3′ and 5′-CAAAGTTGTCATGGATGACC-3′ for *GAPDH*.

Results

HGF enhances Shh-induced medulloblastoma formation by stimulating proliferation and survival of neural progenitor cells

To investigate the role of HGF in medulloblastoma formation, we used the RCAS/*tv-a* somatic cell gene transfer system to express HGF and Shh ectopically in the postnatal mouse

cerebellum. Animals showing increased head circumference (a sign of internal hydrocephalus) or debilitation were sacrificed and analyzed immediately. All remaining mice were sacrificed for analysis 12 weeks after injection. To assess tumor formation, the brains were dissected, sectioned, and stained with hematoxylin and eosin. Medulloblastomas were detected in 16 of 41 mice injected with RCAS-Shh alone (39%), consistent with the known ability of hyperactive Shh signaling to induce medulloblastomas. Tumor incidence increased twofold in mice injected with RCAS-Shh and RCAS-HGF in combination (32 of 41=78%; P=0.0003 by χ^2 contingency test). No tumors developed in mice that were injected with RCAS-HGF alone.

The tumors arose in the dorsolateral cerebellum at the injection sites (Fig. 1*A*). Microscopically, the tumors induced by Shh and Shh+HGF contained regions of densely packed sheets of cells with hyperchromatic nuclei and scant cytoplasm, resembling the classical type of medulloblastoma in humans. Immunoperoxidase staining showed that the tumor cells expressed βIII tubulin and NeuN, markers of early neuronal differentiation, but they did not express neurofilament protein, a marker for terminally differentiated neurons. GFAP expression was present in the abundant glial processes coursing throughout the tumor stroma. Some of the tumors contained microscopic nodules, in which cell density and proliferation (as measured by Ki67 immunostaining) were increased compared with adjacent areas of uniformly distributed tumor cells (Fig. 1*B*—*C*). The cells inside these hyperplastic nodules did not express neuronal markers NeuN, synaptophysin, or βIII tubulin (Fig. 1*D*).

Neuronal differentiation in the mouse tumors often occurred in discrete foci, a pattern similar to that seen in human medulloblastomas of the nodular/desmoplastic subtype, which are associated with Hedgehog signaling activity. In some animals, the regions of neuronal differentiation were quite large, similar to those described in another variant called medulloblastoma with extensive nodularity (MBEN) (28). The fibrillar neuropil had a streaming quality in these highly differentiated regions and contained clusters and rows of neurocytic cells with round nuclei (Fig. 2*A*). In contrast to the hyperplastic nodules or regions showing the classical histological pattern, the MBEN-like areas had low cell density, little proliferation, and positive immunoreactive staining for neuronal differentiation markers βIII tubulin, synaptophysin, and NeuN (Fig. 2*B*). Also present in most tumors were smaller zones of neuronal differentiation associated with cell cycle exit, interspersed between zones containing proliferating, undifferentiated tumor cells (Fig. 2*C*).

To verify *in vivo* expression of genes transferred via RCAS vectors, we demonstrated specific staining of tumor cells with antibodies directed against epitope tags appended to the encoded proteins. Figure 3*A* shows positive staining for HA-tagged Shh and Myc-tagged HGF in the cytoplasm of tumor cells. The anti-Myc antibody 9E10 showed a higher level of background staining in the cerebellum than the anti-HA antibody F7. To provide additional evidence for *in vivo* expression of retroviral HGF, we carried out RT/PCR analysis of 15 brain specimens from mice that were injected with RCAS-Shh and RCAS-HGF and sacrificed at the onset of neurological signs. We used oligonucleotide primers that were complementary to human *HGF* sequences present in the RCAS vector but not present in endogenous mouse *Hgf*. Three specimens were excluded from further analysis because a parallel PCR reaction indicated that contaminating DNA was present. A reaction product corresponding to human *HGF* mRNA was detected in 9 of the remaining 12 specimens, indicating that RCAS-transferred *HGF* was expressed (Fig. 3*B*).

We reported previously that Shh-induced medulloblastoma formation in mice can be enhanced by overexpressing the antiapoptotic protein Bcl-2 (11) or by stimulating PI3K signaling with IGF-II or its downstream effector molecule Akt (9). We attributed the enhancing effect of Bcl-2 to expansion of Shh-stimulated cells, which might otherwise be eliminated by compensatory activation of intrinsic cell death programs. The growth advantage provided by IGF-II and Akt

was derived from the well-known ability of PI3K pathway activation to stimulate both cell cycle progression and cell survival. Because HGF has overlapping positive effects on cell cycle progression and survival in many cell types, we asked whether HGF was enhancing medulloblastoma growth by supplementing Shh-stimulated proliferation or by additionally blocking apoptosis. To address this question, we measured the percentage of tumor cells advancing through the cell cycle by immunostaining tumor-bearing brain sections with an antibody that detects Ki67, a protein expressed during cell cycle phases G_1-M. Figure 4*A* shows that the mean proliferation index of Shh-induced medulloblastomas (17%) was greatly enhanced by coexpression of HGF (39%) ($P<0.0001$). Moreover, the mitogenic effect of HGF was more potent than we reported previously for IGF-II and an activated, transforming allele of Akt (9,11).

To assess the effect of RCAS-mediated HGF expression on apoptosis, we carried out immunoperoxidase staining of tumors using an antibody that specifically recognizes the active proteolytic fragment of caspase-3 (cleaved caspase-3). As shown in Figure 4*B*, the percentage of cells positive for cleaved caspase-3 (apoptotic index) was lower in medulloblastomas induced by Shh+HGF (0.9%) than in tumors induced by Shh alone (1.4%) ($P<0.0001$). HGF did not suppress apoptosis, however, to levels we achieved with the potent antiapoptotic protein Bcl-2 (0.3%) or with survival factors IGF-II (0.5%) and Akt (0.5%). Taken together, these results indicate that HGF enhanced the growth of Shh-induced medulloblastomas by coordinately stimulating cell cycle progression and suppressing apoptosis. This function is consistent with HGF's dual role as mitogen and survival factor.

Systemic administration of an HGF-neutralizing monoclonal antibody prolongs survival in mice with Shh+HGF—induced medulloblastomas

The enhancing effect of HGF on tumor incidence indicates that HGF cooperates with Shh to transform nestin-expressing cerebellar progenitor cells. If HGF is also involved in maintaining the growth of established tumors, then blocking its action is likely to restrain tumor growth or possibly cause tumor regression. In either case, HGF or its downstream signaling molecules would be rational therapeutic targets for medulloblastoma. Monoclonal antibodies that neutralize growth factors or their receptors are becoming increasingly important anticancer agents (reviewed in (29)). A monoclonal antibody (L2G7) against recombinant human HGF has been shown to neutralize the ability of HGF to stimulate proliferation, scattering, and survival of cells in culture (30). Moreover, systemic administration of L2G7 to mice bearing subcutaneous and intracerebral xenografts of human HGF^+/c-Met^+ glioblastomas prolongs survival and promotes tumor regression (30). Therefore, we examined the effects of L2G7 on medulloblastomas induced by Shh+HGF to confirm the contribution of HGF to tumor growth and to determine the therapeutic efficacy of c-Met pathway inhibitors against medulloblastomas.

To accomplish this, we injected two groups of newborn *Ntv*-a mice with RCAS-Shh and RCAS-HGF to induce medulloblastomas (60 mice per group). Two weeks later, we treated one group by intraperitoneal injection of L2G7 (2.5 mg/kg twice weekly) and a control group with the same dose of an isotype-matched, nonspecific antibody (5G8). We started treatment two weeks after RCAS injection because that was the earliest time point at which we had observed tumors during the three-month tumor induction experiment described above. The primary experimental endpoint was survival time during a four-month observation period. Animals in both groups were monitored daily for signs of hydrocephalus or neurological impairment (gait ataxia or failure to thrive), at the onset of which they were sacrificed and analyzed immediately. All remaining mice were sacrificed four months after the initial RCAS injection. We chose a four-month observation period for the survival study because we noted previously that brain tumors were present in mice that appeared healthy three months after RCAS transfer of Shh

+HGF. The number of experimental animals was calculated based on the 78% incidence of Shh+HGF—induced tumor formation that we observed during a three-month observation period and the assumption that antibody treatment would neutralize the effect of HGF completely.

We used Kaplan-Meier analysis to compare survival times in the two groups. Five mice (3 in the L2G7 group and 2 in the 5G8 group) died from injection-related brain hemorrhage before receiving antibody treatment and were therefore excluded from further analysis. Median survival time was >120 days in the L2G7 group and 73.5 days in the 5G8 control group (P=0.04 by log-rank test) (Fig. 5*A*). Uncensored events (death or euthanasia before study closure) occurred in 26 of 57 (46%) of animals in the L2G7 test group and in 35 of 58 (60%) in the 5G8 control group (P=0.1 by χ^2 contingency test). The survival advantage conferred by systemic L2G7 therapy suggests that sustained HGF expression is a driving force in medulloblastoma growth *in vivo*.

To ascertain that the survival advantage conferred by L2G7 antibody treatment was consequent to HGF blockade rather than off-target effects, we carried out a second survival study of mice injected with RCAS-Shh alone. The experimental protocol was identical to that described above except that the observation time was reduced to three months, the time during which the survival curves diverged in the survival analysis of Shh+HGF—induced tumors. Kaplan-Meier analysis showed no difference in survival between mice treated with L2G7 and mice treated with 5G8 (P=0.5 by log-rank test) (Fig. 5*B*). Thus, the survival benefit afforded by L2G7 therapy to mice with tumors induced by Shh+HGF most likely results from specific inhibition of retrovirus-transduced HGF.

Mechanisms of antitumor activity of anti-HGF antibody L2G7

We carried out a detailed histochemical analysis of the brains from mice treated with L2G7 or 5G8 antibodies in the Shh+HGF survival study (Table 1). The brains were fixed, sectioned, and stained with hematoxylin and eosin. Specimens were scored as positive if they contained tumors large enough to show a clear cytological pattern of medulloblastoma. Tumors were present in 23 of 57 mice in the L2G7 treatment group (40%) and in 34 of 58 mice in the 5G8 control group (59%) (P=0.05 by χ^2 contingency test). Among mice that were scored as uncensored events, tumors were histologically verified in 16 of 26 mice in the L2G7 treatment group (62%) and 26 of 35 mice in the 5G8 control group (74%) (P=0.3). The lower incidence of tumor formation in the presence of L2G7 suggests that HGF cooperates with Shh in the early stages of tumor initiation.

We estimated tumor size by measuring cross-sectional area from transaxial sections through the cerebellum. As shown in Table 1, the mean tumor size was 6.5 mm^2 [95% CI, 4.3–8.7] in the L2G7 groups and 7.6 mm^2 [95% CI, 3.1–12.1] in the 5G8 control group (P=0.7 by unpaired t test). The wide range in tumor size might be explained by variation in the site of tumor origin. That is, small tumors adjacent to critical cerebrospinal fluid pathways can cause obstructive hydrocephalus and early neurological deterioration, whereas tumors arising in the lateral cerebellar hemisphere can grow larger before causing noticeable changes in the animals' neurological conditions.

To assess the effect of HGF inhibition on tumor cell proliferation, we carried out quantitative immunostaining for Ki67 in 14 mice from each treatment group. We analyzed all mice scored as uncensored events in the survival study in which tumors were large enough to count cells in at least ten 40x microscope fields. The proliferation index was equivalent in the two groups (47% for L2G7 compared with 42% for 5G8; P=0.4 by unpaired t test) (Table 1). By contrast, cleaved caspase-3 immunostaining showed that the apoptotic index was increased in tumors

from mice receiving anti-HGF antibody therapy (2.0%) compared with nonspecific antibody (0.6%) ($P<0.0001$).

Angiogenesis is a rate-limiting step in the malignant progression of solid tumors. HGF promotes the essential steps in tumor angiogenesis—extracellular matrix degradation; proliferation, survival, and migration of endothelial cells; and tubule formation. To determine whether suppression of angiogenesis contributed to the inhibitory effect of L2G7 on medulloblastoma growth, we measured microvascular density in Shh+HGF—induced medulloblastomas from mice treated with L2G7 or 5G8 (10 specimens per treatment group). We accomplished this by immunostaining for laminin, a glycoprotein that is expressed in the basement membranes of newly formed and mature blood vessels. The mean microvascular density was equivalent in the two groups (7% for L2G7 compared with 6% for 5G8; $P=0.05$ by unpaired *t* test). Taken together, the results of these comparative histochemical studies indicate that the principle mechanism by which L2G7 therapy exerts its antitumor effect is by eliciting an apoptotic death response in tumor cells.

We carried out a similar histochemical analysis of the mice, in which tumors were induced by Shh alone and then treated with L2G7 or 5G8 antibodies (Supplementary Table 1). We found no significant effect on tumor size, incidence, proliferation, or apoptosis by anti-HGF antibody treatment, indicating that the antitumor effects of L2G7 are most likely consequent to specific inhibition of HGF/c-Met signaling.

Discussion

Using the RCAS/*tv-a* gene transfer system, we previously identified proteins belonging to different functional classes that cooperate with Shh to enhance medulloblastoma formation. These enhancing factors include (a) Myc oncoproteins (5,10), which stimulate proliferation of neural progenitor cells during normal development, (b) Bcl-2, which potently inhibits apoptosis (11), and (c) IGF-II, which concomitantly stimulates proliferation and blocks apoptosis by activating the PI3K signal transduction pathway (9). The findings reported here extend our previous work by identifying HGF as another protein that cooperates with Shh to transform neural progenitor cells and thus initiate medulloblastoma formation. The fact that all of these proteins are highly expressed in human medulloblastomas indicates that their tumor-promoting activity in mice accurately reflects the pathogenesis of the human disease. Moreover, these proteins or their downstream signaling molecules can be considered possible targets for therapeutic intervention.

The ability of HGF to promote medulloblastoma growth reflects the role of HGF/c-Met signaling during normal cerebellar development. Mouse embryos that are nullizygous for *Hgf* or *c-Met* develop lethal defects in the placenta, liver, and skeletal muscles (reviewed in (31)). Mice engineered to carry a hypomorphic *c-Met* allele that impaired the ability of the encoded receptor to activate mitogen-activated protein kinase (MAPK) signaling were viable, but these mice developed small, abnormally foliated cerebella (24). In these c-Met signaling mutants, cerebellar hypoplasia resulted from blunting of the normally robust proliferation of granule neuron precursors in early postnatal development. Thus, the enhanced proliferation we observed in Shh+HGF—induced medulloblastomas (Fig. 4*A*) is a pathological manifestation of the physiological role of HGF in stimulating proliferation of neural progenitors during normal cerebellar development. We also observed a strong antiapoptotic effect of HGF in Shh +HGF—induced medulloblastomas. This prosurvival effect is consistent with the neuroprotection afforded by HGF to cerebellar granule neurons in culture, an effect that is mediated by the ability of HGF to activate PI3K signaling (23,32).

Previous studies have shown that HGF stimulates human medulloblastoma cell lines to proliferate in culture and enhances colony formation in semisolid media (22). Furthermore, forced overexpression of HGF in the well-studied medulloblastoma cell line DAOY enhances growth of both subcutaneous and intracerebral xenografts in athymic mice. A limitation of these xenograft models is that long-term propagation of tumor cells in culture can select for mutations that are not tumor-initiating events *in vivo*. The findings we report here strengthen and advance the cell culture work because they show that HGF cooperates with Shh to transform cerebellar neuron progenitors and initiate medulloblastoma formation *in vivo*. The fact that the tumorigenic effect of HGF was observed in immunocompetent mice further increases the extent to which our model system parallels the human disease.

A novel feature of our mouse model of Shh-induced medulloblastoma is that it recapitulates the pathobiology of neuronal differentiation found in human tumors. The nodular/desmoplastic medulloblastoma subtype is characterized by small islands of cells that have stopped proliferating and undergone neuronal differentiation (33). Mutations that activate Hedgehog signaling, as well as gene expression signatures associated with that pathway, are more common in the nodular/desmoplastic subtype than in the classical subtype (34). Accurate modeling of such features in mice is clinically relevant because a central therapeutic objective is to force tumor cells to exit the cell cycle and differentiate.

Multiple approaches have been taken to inhibit HGF/c-Met signaling in tumor cells. These include blocking HGF and c-Met with monoclonal antibodies (22,35-37), antagonizing c-Met by truncated HGF peptides (38,39) or decoy receptors (40), preventing receptor dimerization with a c-Met Sema domain peptide (41), suppressing expression of HGF and c-Met with ribozymes (42,43), and inhibiting c-Met tyrosine kinase activity using small molecules (44-46). Our observation that the HGF-neutralizing antibody L2G7 prolongs survival in mice with medulloblastomas induced by Shh+HGF not only validates the tumorigenic effect of HGF but also suggests that HGF might be a feasible treatment target.

Several observations indicate that response to anti-HGF therapy was incomplete, at least under the conditions of these experiments. First, cumulative survival of mice with Shh+HGF—induced tumors continued to fall in the L2G7 treatment group throughout the four-month observation time. Second, brain tumors were found in censored cases (asymptomatic mice) at the close of the study (6 of 31 mice in the L2G7 group and 8 of 23 in the 5G8 group). Third, L2G7 antibody treatment did not suppress tumor cell proliferation even though it stimulated apoptosis. It is possible that treatment response could be enhanced by increasing the dosage or duration of antibody therapy. Sustained proliferation in the presence of HGF-blocking antibody could also be driven by unchecked Shh stimulation. This possibility suggests that medulloblastoma growth could be suppressed further by combining anti-HGF antibodies with compounds that inhibit Shh/Patched signaling, like cyclopamine analogs, which have been shown to inhibit medulloblastoma growth in Patched-deficient mice (7).

The fact that L2G7 treatment induces tumor cell apoptosis but does not block HGF-induced proliferation is consistent with a mechanism whereby tumors that develop in response to Shh +HGF become addicted to an HGF-driven survival pathway, which is not active in Shh-induced tumors. This addiction is unmasked by HGF/c-Met pathway inhibition as evidenced by the increase in apoptosis in response to L2G7 antibody treatment. We cannot exclude the possibility that L2G7 might induce apoptosis via a mechanism distinct from preventing c-Met activation. Nevertheless, the fact that apoptotic indices are comparable in Shh—induced tumors from mice treated with L2G7 or 5G8 (Supplementary Table 1) and from untreated mice (Fig. 4*B*) argues against this possibility.

The curves shown in Figure 5*A* indicate that cumulative survival drops off rapidly during the first 30 days after retroviral transfer of Shh+HGF. It is during this time period that the protective effect of L2G7 appears greatest. This indicates that the efficacy of HGF blockade diminishes with continued exposure to the L2G7 antibody. This phenomenon could be explained by acquisition of secondary genetic mutations that drive tumor growth through ligand-independent mechanisms, like c-Met activation. In support of this mechanism, somatically acquired mutations that stimulate the tyrosine kinase activity of c-Met are found in various types of human tumors (12).

Systemic treatment with L2G7, the antibody used in our study, has also been shown to induce regression of human glioblastoma xenografts (U87 cells) implanted intracranially into immunodeficient mice and to prolong survival of tumor-bearing mice (30). A different monoclonal antibody (AMG 102) was shown to promote regression of subcutaneously implanted U87 xenografts, and therapeutic response to AMG102 was enhanced by concurrent chemotherapy (35,47). The results that we present here comprise an important advance in neuro-oncology not only because they broaden the spectrum of brain tumor types that respond to anti-HGF therapy but also because they demonstrate efficacy in a preclinical mouse model in which invasive tumors arise endogenously.

There is a pressing need to identify novel treatment targets for medulloblastomas, especially for children <3 years of age, for whom the toxic effects of radiation on the developing nervous system are unacceptable. A practical challenge for pediatric oncologists treating malignant brain tumors in infants is to suppress tumor growth during critical stages of neurological development, after which radiotherapy can be used with less risk of long-term neurocognitive impairment. Currently, preirradiation chemotherapy is used for this purpose, but response rates are low. For example, the Children's Cancer Group reported a three-year, progression-free survival rate of only 22% in children <3 years of age treated with an eight-drug, postsurgical, preirradiation regimen (48). Numerous agents designed to target HGF or c-Met have recently entered clinical trials for cancer. The ability of anti-HGF monoclonal antibody therapy to prolong survival in our preclinical mouse model suggests that targeting the HGF/c-Met pathway might be a useful adjunct to preirradiation chemotherapy for suppressing medulloblastoma growth in young children.

Supplementary Material

Refer to Web version on PubMed Central for supplementary material.

ACKNOWLEDGMENTS

We thank Dr. Kenneth Boucher and Dr. Jay Riva-Cambrin for help with statistical analysis and Kristin Kraus for editorial assistance.

GRANT SUPPORT: This work was supported by NIH CA108622 (D.W.F.), NS43987 (J.L.), and CA129192 (J.L.).

References

1. Rood BR, Macdonald TJ, Packer RJ. Current treatment of medulloblastoma: recent advances and future challenges. Semin Oncol 2004;31:666–75. [PubMed: 15497120]
2. Gajjar A, Chintagumpala M, Ashley D, et al. Risk-adapted craniospinal radiotherapy followed by high-dose chemotherapy and stem-cell rescue in children with newly diagnosed medulloblastoma (St Jude Medulloblastoma-96): long-term results from a prospective, multicentre trial. Lancet Oncol 2006;7:813–20. [PubMed: 17012043]
3. Goodrich LV, Scott MP. Hedgehog and patched in neural development and disease. Neuron 1998;21:1243–57. [PubMed: 9883719]

4. Weiner HL, Bakst R, Hurlbert MS, et al. Induction of medulloblastomas in mice by sonic hedgehog, independent of Gli1. Cancer Res 2002;62:6385–9. [PubMed: 12438220]
5. Rao G, Pedone CA, Coffin CM, Holland EC, Fults DW. c-Myc enhances Sonic hedgehog-induced medulloblastoma formation from nestin-expressing neural progenitors in mice. Neoplasia 2003;5:198–204. [PubMed: 12869303]
6. Hallahan AR, Pritchard JI, Hansen S, et al. The SmoA1 mouse model reveals that notch signaling is critical for the growth and survival of sonic hedgehog-induced medulloblastomas. Cancer Res 2004;64:7794–800. [PubMed: 15520185]
7. Romer JT, Kimura H, Magdaleno S, et al. Suppression of the Shh pathway using a small molecule inhibitor eliminates medulloblastoma in Ptc1(+/-) p53(-/-) mice. Cancer Cell 2004;6:229–40. [PubMed: 15380514]
8. Wetmore C, Eberhart DE, Curran T. Loss of *p53* but not *ARF* accelerates medulloblastoma in mice heterozygous for *patched*. Cancer Res 2001;61:513–6. [PubMed: 11212243]
9. Rao G, Pedone CA, Del Valle L, Reiss K, Holland EC, Fults DW. Sonic hedgehog and insulin-like growth factor signaling synergize to induce medulloblastoma formation from nestin-expressing neural progenitors in mice. Oncogene 2004;23:6156–62. [PubMed: 15195141]
10. Browd SR, Kenney AM, Gottfried ON, et al. N-myc can substitute for insulin-like growth factor signaling in a mouse model of sonic hedgehog-induced medulloblastoma. Cancer Res 2006;66:2666–72. [PubMed: 16510586]
11. McCall TD, Pedone CA, Fults DW. Apoptosis suppression by somatic cell transfer of Bcl-2 promotes Sonic hedgehog-dependent medulloblastoma formation in mice. Cancer Res 2007;67:5179–85. [PubMed: 17545597]
12. Birchmeier C, Birchmeier W, Gherardi E, Vande Woude GF. Met, metastasis, motility and more. Nat Rev Mol Cell Biol 2003;4:915–25. [PubMed: 14685170]
13. Abounader R, Laterra J. Scatter factor/hepatocyte growth factor in brain tumor growth and angiogenesis. Neuro-oncol 2005;7:436–51. [PubMed: 16212809]
14. Takayama H, LaRochelle WJ, Sharp R, et al. Diverse tumorigenesis associated with aberrant development in mice overexpressing hepatocyte growth factor/scatter factor. Proc Natl Acad Sci U S A 1997;94:701–6. [PubMed: 9012848]
15. Bottaro DP, Rubin JS, Faletto DL, et al. Identification of the hepatocyte growth factor receptor as the c-met proto-oncogene product. Science 1991;251:802–4. [PubMed: 1846706]
16. Jeffers M, Fiscella M, Webb CP, Anver M, Koochekpour S, Vande Woude GF. The mutationally activated Met receptor mediates motility and metastasis. Proc Natl Acad Sci U S A 1998;95:14417–22. [PubMed: 9826715]
17. Liang TJ, Reid AE, Xavier R, Cardiff RD, Wang TC. Transgenic expression of tpr-met oncogene leads to development of mammary hyperplasia and tumors. J Clin Invest 1996;97:2872–7. [PubMed: 8675700]
18. Wang R, Ferrell LD, Faouzi S, Maher JJ, Bishop JM. Activation of the Met receptor by cell attachment induces and sustains hepatocellular carcinomas in transgenic mice. J Cell Biol 2001;153:1023–34. [PubMed: 11381087]
19. Rosen EM, Laterra J, Joseph A, et al. Scatter factor expression and regulation in human glial tumors. Int J Cancer 1996;67:248–55. [PubMed: 8760595]
20. Koochekpour S, Jeffers M, Rulong S, et al. Met and hepatocyte growth factor/scatter factor expression in human gliomas. Cancer Res 1997;57:5391–8. [PubMed: 9393765]
21. Abounader R, Ranganathan S, Lal B, et al. Reversion of human glioblastoma malignancy by U1 small nuclear RNA/ribozyme targeting of scatter factor/hepatocyte growth factor and c-met expression. J Natl Cancer Inst 1999;91:1548–56. [PubMed: 10491431]
22. Li Y, Lal B, Kwon S, et al. The scatter factor/hepatocyte growth factor: c-met pathway in human embryonal central nervous system tumor malignancy. Cancer Res 2005;65:9355–62. [PubMed: 16230398]
23. Hossain MA, Russell JC, Gomez R, Laterra J. Neuroprotection by scatter factor/hepatocyte growth factor and FGF-1 in cerebellar granule neurons is phosphatidylinositol 3-kinase/akt-dependent and MAPK/CREB-independent. J Neurochem 2002;81:365–78. [PubMed: 12064484]

24. Ieraci A, Forni PE, Ponzetto C. Viable hypomorphic signaling mutant of the Met receptor reveals a role for hepatocyte growth factor in postnatal cerebellar development. Proc Natl Acad Sci U S A 2002;99:15200–5. [PubMed: 12397180]
25. Holland EC, Hively WP, DePinho RA, Varmus HE. A constitutively active epidermal growth factor receptor cooperates with disruption of G1 cell-cycle arrest pathways to induce glioma-like lesions in mice. Genes Dev 1998;12:3675–85. [PubMed: 9851974]
26. Fogarty MP, Kessler JD, Wechsler-Reya RJ. Morphing into cancer: the role of developmental signaling pathways in brain tumor formation. J Neurobiol 2005;64:458–75. [PubMed: 16041741]
27. Federspiel MJ, Bates P, Young JAT, Varmus HE, Hughes SH. A system for tissue-specific gene targeting: transgenic mice susceptible to subgroup A avian leukosis virus-based retroviral vectors. Proc Natl Acad Sci U S A 1994;91:11241–5. [PubMed: 7972042]
28. Giangaspero F, Perilongo G, Fondelli MP, et al. Medulloblastoma with extensive nodularity: a variant with favorable prognosis. J Neurosurg 1999;91:971–7. [PubMed: 10584843]
29. Adams GP, Weiner LM. Monoclonal antibody therapy of cancer. Nat Biotechnol 2005;23:1147–57. [PubMed: 16151408]
30. Kim KJ, Wang L, Su YC, et al. Systemic anti-hepatocyte growth factor monoclonal antibody therapy induces the regression of intracranial glioma xenografts. Clin Cancer Res 2006;12:1292–8. [PubMed: 16489086]
31. Maina F, Klein R. Hepatocyte growth factor, a versatile signal for developing neurons. Nat Neurosci 1999;2:213–7. [PubMed: 10195212]
32. Zhang L, Himi T, Morita I, Murota S. Hepatocyte growth factor protects cultured rat cerebellar granule neurons from apoptosis via the phosphatidylinositol-3 kinase/Akt pathway. J Neurosci Res 2000;59:489–96. [PubMed: 10679787]
33. Eberhart CG, Kaufman WE, Tihan T, Burger PC. Apoptosis, neuronal maturation, and neurotrophin expression within medulloblastoma nodules. J Neuropathol Exp Neurol 2001;60:462–9. [PubMed: 11379821]
34. Pomeroy SL, Tamayo P, Gaasenbeek M, et al. Prediction of central nervous system embryonal tumour outcome based on gene expression. Nature 2002;415:436–42. [PubMed: 11807556]
35. Burgess T, Coxon A, Meyer S, et al. Fully human monoclonal antibodies to hepatocyte growth factor with therapeutic potential against hepatocyte growth factor/c-Met-dependent human tumors. Cancer Res 2006;66:1721–9. [PubMed: 16452232]
36. Cao B, Su Y, Oskarsson M, et al. Neutralizing monoclonal antibodies to hepatocyte growth factor/scatter factor (HGF/SF) display antitumor activity in animal models. Proc Natl Acad Sci U S A 2001;98:7443–8. [PubMed: 11416216]
37. Martens T, Schmidt NO, Eckerich C, et al. A novel one-armed anti-c-Met antibody inhibits glioblastoma growth in vivo. Clin Cancer Res 2006;12:6144–52. [PubMed: 17062691]
38. Brockmann MA, Papadimitriou A, Brandt M, Fillbrandt R, Westphal M, Lamszus K. Inhibition of intracerebral glioblastoma growth by local treatment with the scatter factor/hepatocyte growth factor-antagonist NK4. Clin Cancer Res 2003;9:4578–85. [PubMed: 14555533]
39. Tomioka D, Maehara N, Kuba K, et al. Inhibition of growth, invasion, and metastasis of human pancreatic carcinoma cells by NK4 in an orthotopic mouse model. Cancer Res 2001;61:7518–24. [PubMed: 11606388]
40. Michieli P, Mazzone M, Basilico C, et al. Targeting the tumor and its microenvironment by a dual-function decoy Met receptor. Cancer Cell 2004;6:61–73. [PubMed: 15261142]
41. Kong-Beltran M, Stamos J, Wickramasinghe D. The Sema domain of Met is necessary for receptor dimerization and activation. Cancer Cell 2004;6:75–84. [PubMed: 15261143]
42. Abounader R, Lal B, Luddy C, et al. In vivo targeting of SF/HGF and c-met expression via U1snRNA/ribozymes inhibits glioma growth and angiogenesis and promotes apoptosis. FASEB J 2002;16:108–10. [PubMed: 11729097]
43. Kim SJ, Johnson M, Koterba K, Herynk MH, Uehara H, Gallick GE. Reduced c-Met expression by an adenovirus expressing a c-Met ribozyme inhibits tumorigenic growth and lymph node metastases of PC3-LN4 prostate tumor cells in an orthotopic nude mouse model. Clin Cancer Res 2003;9:5161–70. [PubMed: 14613995]

44. Wang X, Le P, Liang C, et al. Potent and selective inhibitors of the Met [hepatocyte growth factor/scatter factor (HGF/SF) receptor] tyrosine kinase block HGF/SF-induced tumor cell growth and invasion. Mol Cancer Ther 2003;2:1085–92. [PubMed: 14617781]

45. Christensen JG, Schreck R, Burrows J, et al. A selective small molecule inhibitor of c-Met kinase inhibits c-Met-dependent phenotypes in vitro and exhibits cytoreductive antitumor activity in vivo. Cancer Res 2003;63:7345–55. [PubMed: 14612533]

46. Bellon SF, Kaplan-Lefko P, Yang Y, et al. c-Met inhibitors with novel binding mode show activity against several hereditary papillary renal cell carcinoma-related mutations. J Biol Chem 2008;283:2675–83. [PubMed: 18055465]

47. Jun HT, Sun J, Rex K, et al. AMG 102, a fully human anti-hepatocyte growth factor/scatter factor neutralizing antibody, enhances the efficacy of temozolomide or docetaxel in U-87 MG cells and xenografts. Clin Cancer Res 2007;13:6735–42. [PubMed: 18006775]

48. Geyer JR, Zeltzer PM, Boyett JM, et al. Survival of infants with primitive neuroectodermal tumors or malignant ependymomas of the CNS treated with eight drugs in 1 day: a report from the Childrens Cancer Group. J Clin Oncol 1994;12:1607–15. [PubMed: 8040673]

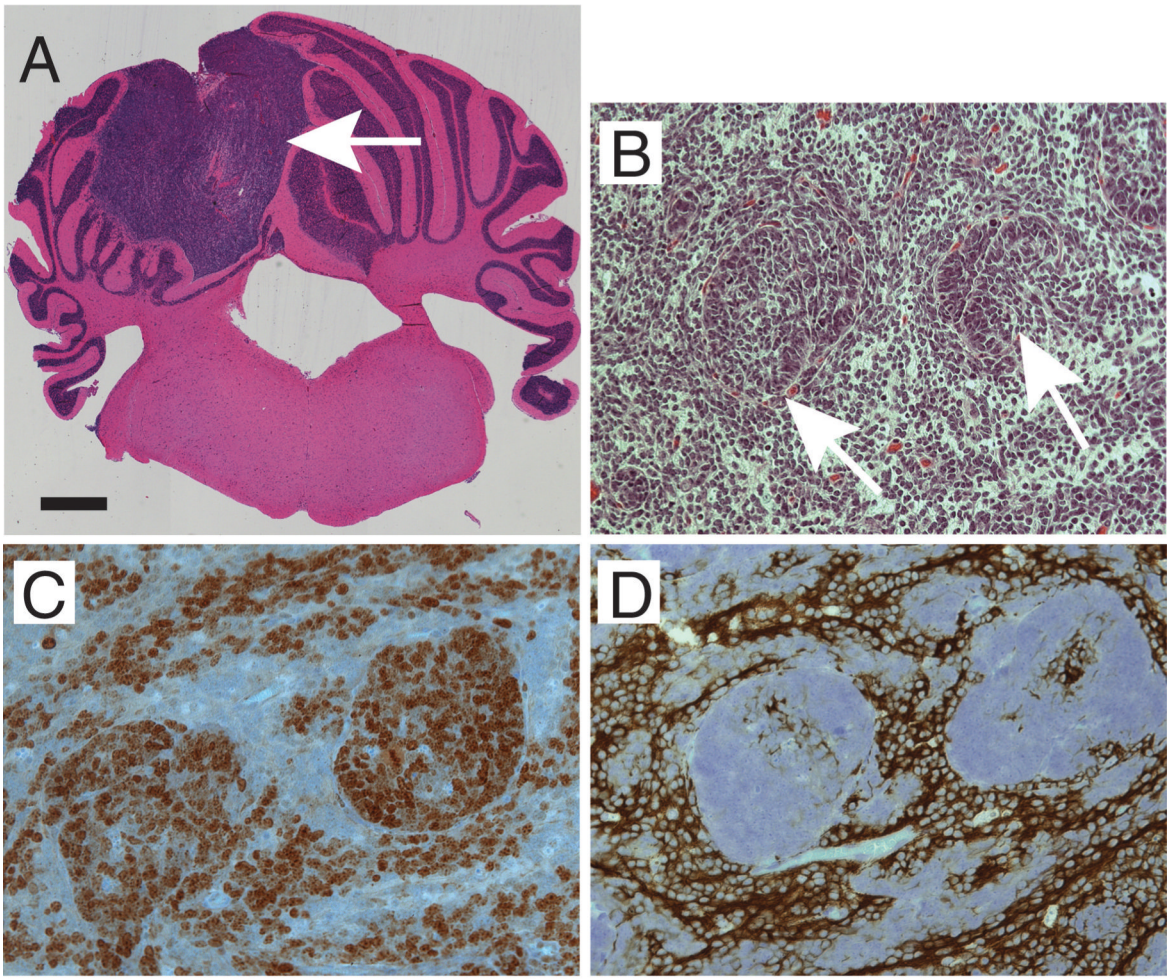

Figure 1.
Histopathology of medulloblastomas induced by Shh+HGF. *A*, coronal brain section showing tumor (*arrow*) in the dorsolateral cerebellum (H&E). *B*, microscopic pattern showing nodules of increased cell density (*arrows*) (H&E). *C—D*, immunoperoxidase staining showing that tumor cells inside the hyperplastic nodules are positive for proliferation marker Ki67 (*C*) but negative for neuronal marker βIII tubulin (*D*) compared with adjacent tumor areas. *Scale bars*, 500 μm (*A*), 50 μm (*B—D*).

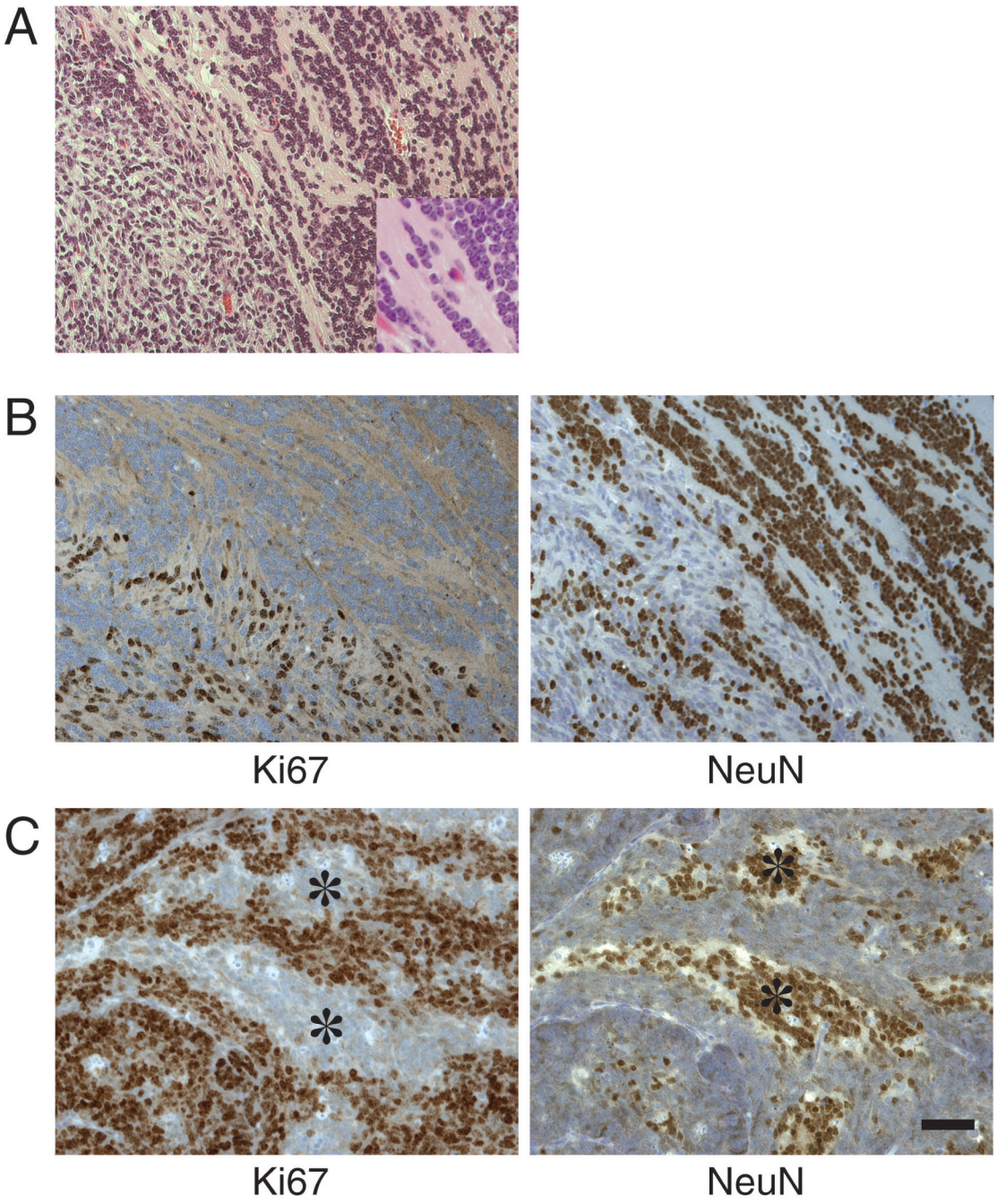

Figure 2.

Histopathology of Shh+HGF—induced medulloblastoma with streaming neuropil pattern. *A*, streaming neuropil histological pattern, in which round, neurocytic-appearing tumor cells are arrayed in a linear pattern (*upper right and inset*) adjacent to an area of disorganized cytoarchitecture (*lower left*) (H&E). *B*, immunoperoxidase staining showing that the streaming neuropil areas (*upper right*) lack Ki67 staining but show abundant immunoreactivity for neuronal differentiation marker NeuN. *C*, smaller regions of cell cycle exit and neuronal differentiation marked by decreased Ki67 and increased NeuN were also common (*asterisks*). *Scale bar*, 50 μm.

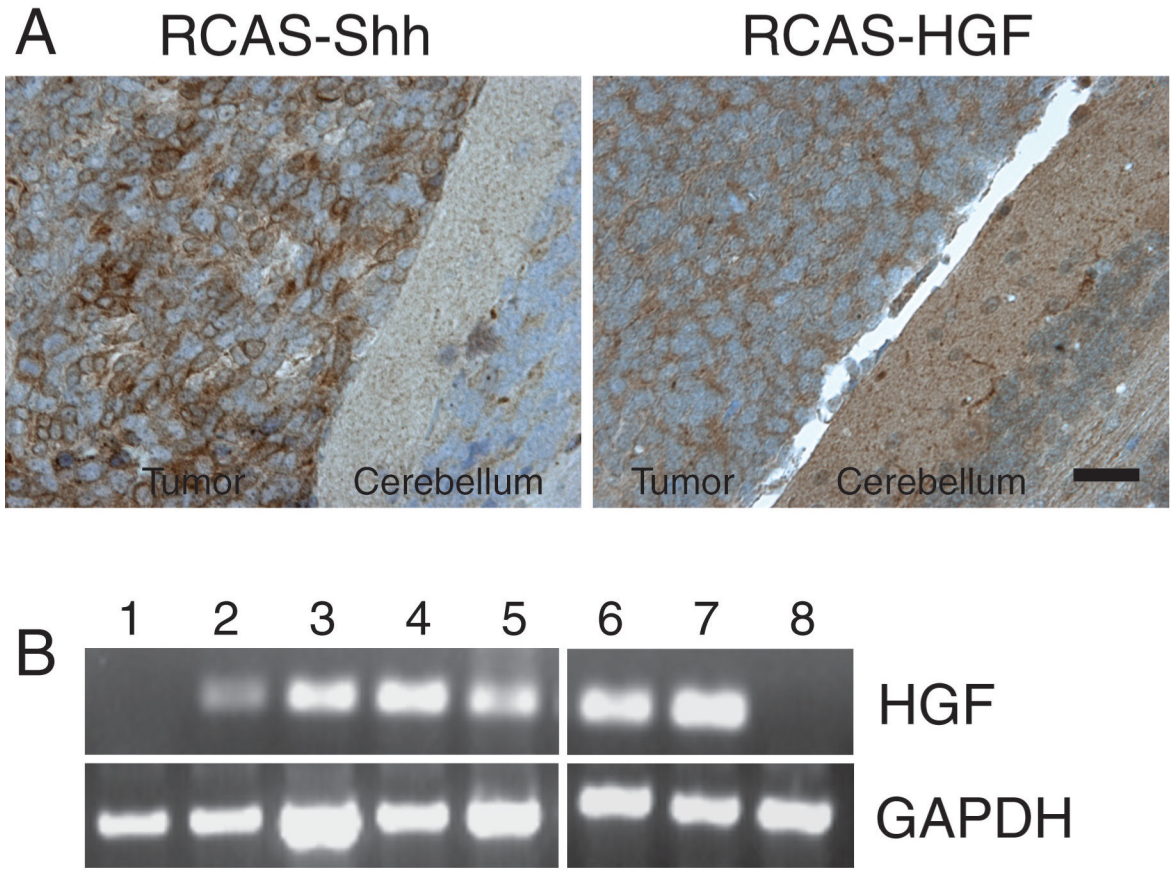

Figure 3.

Expression of RCAS retrovirus—transferred Shh and HGF in tumor cells. *A*, immunoperoxidase staining of medulloblastoma induced by RCAS-mediated transfer of HA-tagged Shh and Myc-tagged HGF. F7 antibody against the HA epitope detects expression of retroviral Shh and 9E10 antibody detects expression of retroviral HGF in the cytoplasm of tumor cells. *Scale bar*, 25 μm. *B*, RT-PCR analysis of human *HGF* sequences in cerebella from mice injected with RCAS-Shh and RCAS-HGF (*lanes 1–7*) and uninjected mouse (*lane 8*). Reaction products indicate expression of human *HGF* from the integrated RCAS provirus (*lanes 2–7*). Absence of a product in *lane 1* demonstrates that RCAS injection did not lead to productive viral infection in all mice.

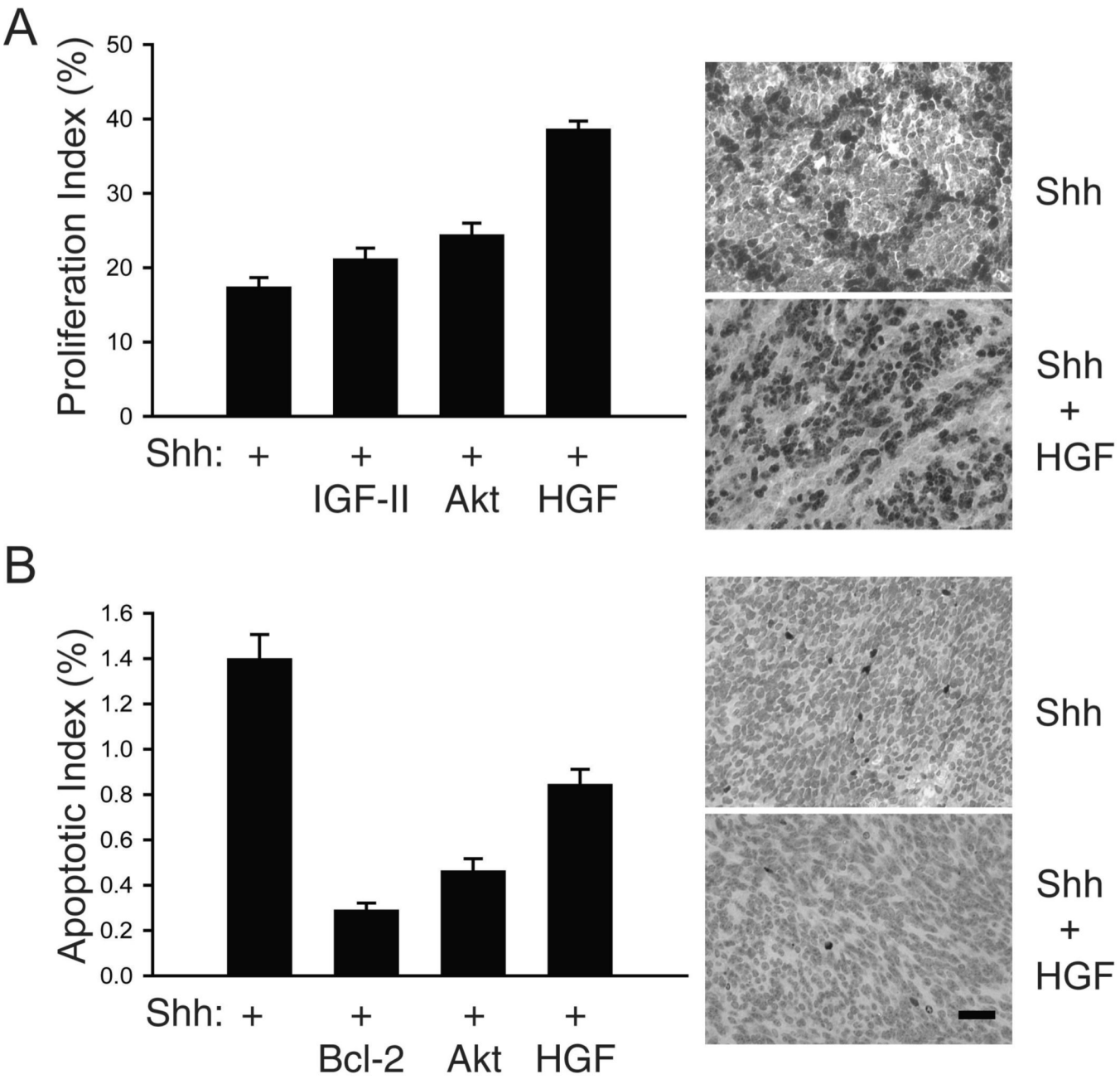

Figure 4.

Analysis of proliferation and apoptosis in Shh+HGF—induced medulloblastomas. Bar graphs and representative photomicrographs showing the percentage of tumor cells with positive immunoreactive staining for Ki67 (proliferation index) (*A*) and cleaved caspase-3 (apoptotic index) (*B*) in medulloblastomas induced by RCAS-mediated transfer of Shh alone or in combination with IGF-II, Akt, Bcl-2, and HGF. *Columns*, means; *error bars*, SEM. *Scale bar*, 25 μm.

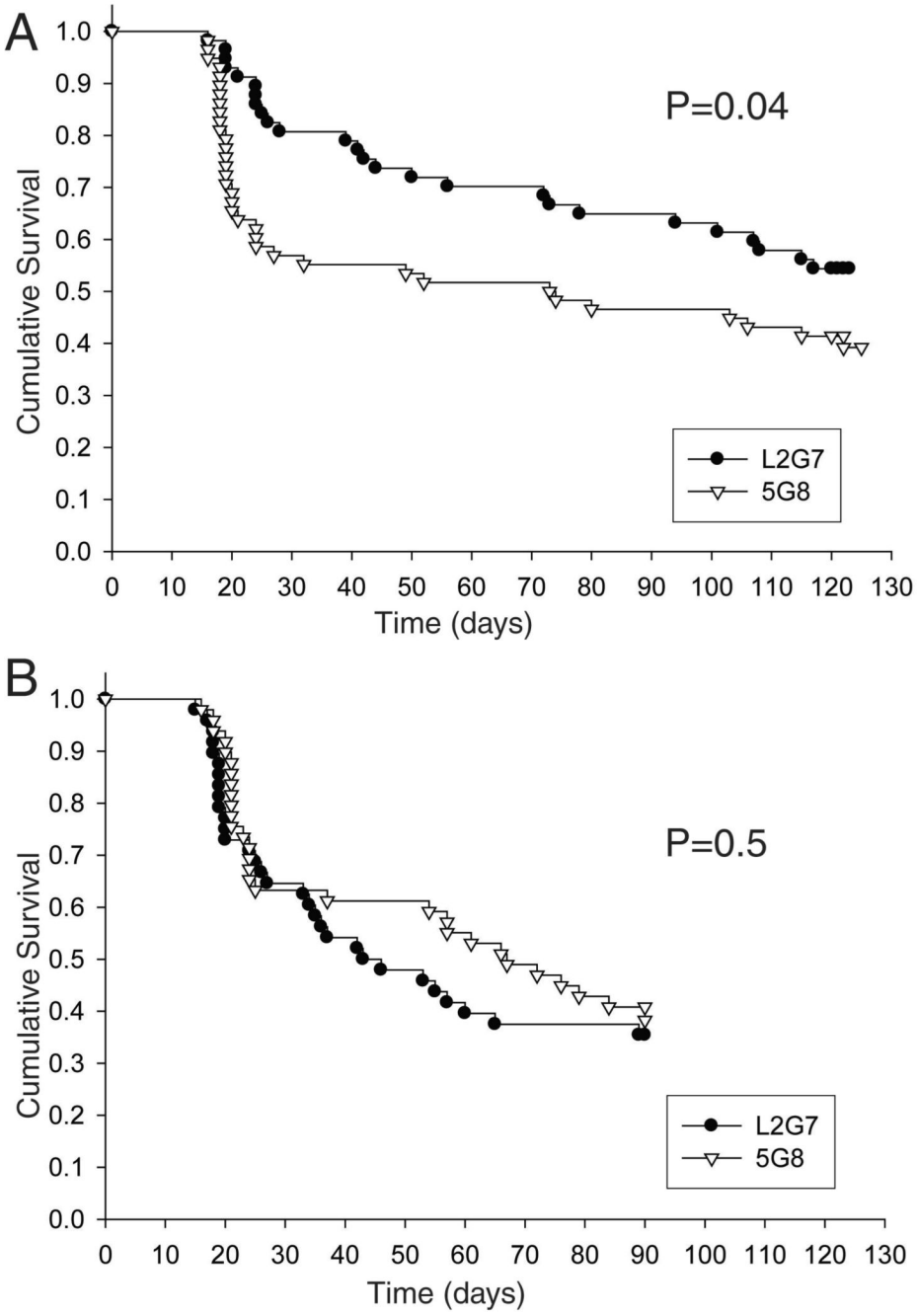

Figure 5.

Preclinical testing of anti-HGF monoclonal antibody L2G7 in mice with medulloblastomas. Kaplan-Meier survival analysis of mice injected with RCAS-Shh and RCAS-HGF (*A*) or RCAS-Shh alone (*B*) on day 0 and then treated with HGF-specific monoclonal antibody L2G7 or nonspecific control antibody 5G8 starting on day 14. *P* values were derived from the log-rank test.

Table 1

Analysis of Shh+HGF—induced medulloblastomas in mice after systemic antibody treatment

	L2G7	5G8	*P* value
Tumor incidence (4 months)	23 of 57 (40%)	34 of 58 (59%)	0.05
Tumor size (mm^2)*	6.5	7.6	0.7
Proliferation index (%)*	47	42	0.4
Apoptotic index (%)*	2.0	0.6	<0.0001
Microvascular density (%)*	7	6	0.05

* Mean values